J Fluoresc (2010) 20:27–35
DOI 10.1007/s10895-009-0518-3

ORIGINAL PAPER

Photobleaching-Based Quantitative Analysis of Fluorescence Resonance Energy Transfer inside Single Living Cell

Longxiang Wang · Tongsheng Chen · Junle Qu · Xunbin Wei

Received: 8 January 2009 / Accepted: 2 July 2009 / Published online: 9 July 2009

Abstract The current advances of fluorescence microscopy and new fluorescent probes make fluorescence resonance energy transfer (FRET) a powerful technique for studying protein-protein interactions inside living cells. It is very hard to quantitatively analyze FRET efficiency using intensity-based FRET imaging microscopy due to the presence of autofluorescence and spectral crosstalks. In this study, we for the first time developed a novel photobleaching-based method to quantitatively detect FRET efficiency (Pb-FRET) by selectively photobleaching acceptor. The Pb-FRET method requires two fluorescence detection channels: a donor channel (CH_1) to selectively detect the fluorescence from donor, and a FRET channel (CH_2) which normally includes the fluorescence from both acceptor and donor due to emission spectral crosstalk. We used the Pb-FRET method to quantitatively measure the FRET efficiency of SCAT3, a caspase-3 indicator based on FRET, inside single living cells stably expressing SCAT3 during STS-induced apoptosis. At 0, 6 and 12 h after STS treatment, the FRET efficiency of SCAT3 obtained by Pb-FRET inside living cells was verified by two-photon excitation (TPE) fluorescence lifetime imaging microscopy (FLIM). The temporal resolution of Pb-FRET method is in second time-scale for ROI photobleaching, even in microsecond time-scale for spot photobleaching. Our results demonstrate that the Pb-FRET method is independent of photobleaching degree, and is very useful for quantitatively monitoring protein-protein interactions inside single living cell.

Keywords Fluorescence resonance energy transfer (FRET) · Photobleaching acceptor · Caspase-3 · Fluorescene lifetime imaging microscopy (FLIM)

L. Wang · T. Chen (✉)
MOE Key laboratory of Laser Life Science
& Institute of Laser Life Science, South China Normal University,
Guangzhou 510631, China
e-mail: chentsh@scnu.edu.cn

J. Qu
Key Laboratory of Optoelectronic Devices
and Systems of Ministry of Education and Guangdong Province,
Institute of Optoelectronics, Shenzhen University,
Shenzhen 518060, China

X. Wei (✉)
Institutes of Biomedical Sciences, Fudan University,
Shanghai 200032, China
e-mail: xwei@fudan.edu.dn

Introduction

Laser scanning confocal fluorescence microscope (LSCFM) has gained major attraction not only due to their superior sensitivity to environmental properties and its multidimensionality, i.e., its ability to provide various simultaneous readouts (e.g., intensity, anisotropy, spectral characteristics), but also due to their ever-growing range of measurement techniques [1]. There is now widespread interest in the ability to detect protein–protein interactions in living cells using fluorescence resonance energy transfer (FRET) technology. FRET was first described by Förster [2] and has become increasingly important for modern cell biology due to the ability of FRET to measure the distance between molecules on a scale of a few nanometers that is far below the resolution of modern optical far-field microscope [3]. FRET, as a dipole-dipole interaction between neighboring molecules, derives the dependence of the energy transfer efficiency E on the inverse sixth power of intermolecular separation. FRET occurrence should lead to a decrease of the fluorescence intensity of donor and an increase of the fluorescence intensity of acceptor increases [3].

Several FRET microscopy techniques, including sensitized acceptor fluorescence, quenching of donor fluorescence, and donor fluorescence lifetime, have been developed to monitor FRET efficiency [4–7]. For sensitized acceptor fluorescence method, the net FRET signal must be corrected against bleed-through of the fluorescence of non-FRET donor, which requires multiple sets of images, as well as reference samples that contain only one of donor or acceptor fluorophore [8]. FRET efficiency can be also accomplished by comparing the donor fluorescence intensity in the cells transfected with both donor and acceptor fluorescent proteins before and after depleting the acceptor fluorescence by photobleaching [9]. If FRET is present, the fluorescence intensity of donor should increase after acceptor is photobleached [10]. However, it is difficult to photobleach all of the acceptor molecules, and long-time photobleaching may cause a serious damage to the living cell [11]. Measurement of the fluorescence lifetime of donor by fluorescence lifetime imaging microscope (FLIM), which is very expensive and not widely available, is an alternative method to quantitatively obtain FRET efficiency, but both photobleaching and photoconversion might contribute to the decrease of the fluorescence lifetime of donor, which could invalidate FRET measurements [12]. Many correction algorithms have been proposed to quantitatively analyze FRET efficiency [13–15].

Apoptosis, one of the programmed cell death (PCD), is a highly ordered form of cell suicide [16], and its biochemical process is activated via two well-studied pathways: death receptor-mediated pathway and mitochondria-mediated pathway. Activation of casepase-3 is considered to be the final step in many apoptosis pathways [17]. In an attempt to detect the caspase-3 activation in living cells, Miura et al. constructed SCAT3, a FRET probe that consists of a donor (enhanced cyan fluorescent protein, ECFP) and an acceptor (Venus, a mutant of yellow fluorescent protein) [18]. The donor and the acceptor are linked with a caspase-3 recognition and cleavage sequence (DEVD) [18–20]. The activated caspase-3 cleaves the linker DEVD, and then induces a marked decrease in the FRET efficiency and a significant increase in the lifetime of ECFP. Currently, monitoring the cleavage of SCAT3 is mostly based on the change of the fluorescence intensity ratio of Venus to ECFP [18, 21, 22]. However, quantitative measurement of FRET efficiency is hampered due to the emission and excitation spectra crosstalks.

Staurosporine (STS), used as a positive control on caspase-3 activation study [23–26], is known to be a powerful inducer of apoptosis in variety of cell types. In this study, we for the first time developed a novel photobleaching-based method to quantitatively measure FRET efficiency (Pb-FRET) by selectively photobleaching acceptor. In contrast to the method of photobleaching acceptor [10], Pb-FRET is independent of the bleaching degree,which make it quantitatively obtain FRET efficiency at less bleaching degree. We used Pb-FRET to quantitatively analyze the caspase-3 activation induced by STS. The FRET efficiency of SCTA3 after STS treatment obtained by Pb-FRET method is consistent with the results obtained by fluorescence lifetime imaging microscopy (FLIM) [27, 28]. Our results demonstrate that the Pb-FRET method is independent of the bleaching degree, and is very useful to monitor protein-protein interactions inside single living cell.

Materials and methods

Cell culture

Cells were cultured in DMEM supplemented with 15% fetal calf serum (FCS) with 5% CO_2 at 37 °C in a humidified incubator. Plasmid DNA of *SCAT3* was provided by Dr. Miura [18] (Kiwamu et al., 2003). The cells stably expressing SCAT3 reporter were screened with 0.8 mg/ml G418 [19, 20].

Cell viability assay

The cell viability after STS treatment was measured by CCK-8 assay. Cells were plated in 96-well plates at 5×10^3 cells per well and cultured in the medium with 1 μmol/L STS. At the indicated time points, the cell numbers in five wells were measured as the absorbance (450 nm) of reduced WST-8. Absorbance was measured at 450 nm using auto-microplate reader (infinite M200, Tecan, Austria). All experiments were performed in five wells on three separate occasions (n=3).

Western blotting

The STS treated and untreated cells were lysed in a buffer containing 50 mM Tris–HCl pH 8.0, 150 mM NaCl, 1% Triton X-100, 1 mM Na_3VO_4, 100 mM PMSF and 1_ protease inhibitor cocktail set I (Calbiochem, La Jolla, CA). The samples were separated by 10% SDS–polyacrylamide gel electrophoresis and transferred onto PVDF membrane (Roche, Mannheim, Germany). The resulting membrane was blocked with 5% skim milk, incubated with a designated primary antibody and the secondary antibody. The signals were detected with an ODYSSEY1Infrared Imaging System (LI-COR, Lincoln, NE). The following antibodies were used for immunoblot: the rabbit polyclonal anti-caspase-3 (Cell signaling, Cat. No. 9746), secondary anti-rabbit IgG-HRP (Rockland, Gilbertsville, PA, USA).

Spectral analysis of cells expressing SCAT3 after STS treatment

Cells stably expressing SCAT3 were cultured for 24 hours in 96-well flat-bottomed microtiter plates at 5×10^5 per well in DMEM medium supplemented with 15% fetal calf serum. The emission spectra of the SCAT3 was detected 0, 6, and 12 h after STS treatment by auto-microplate reader (infinite M200, Tecan, Austria), respectively. The excitation wavelength of SCAT3 was 398–438 nm and the emission fluorescence channel was 460–600 nm band-pass.

Two-photon excitation fluorescence lifetime imaging

Fluorescence lifetime of ECFP was measured by two-photon excitation fluorescence lifetime imaging [29, 30]. The method was described in our previous work (Pan et al., 2008). The FLIM data were processed using the SPC Image software (Becker & Hickl GmbH, Germany). For FLIM-FRET measurement, the fluorescence lifetime of the donor alone (τ_D) as well as in the presence of the acceptor (τ_{DA}) are measured, and FRET efficiency can be obtained by $E=1-\tau_{DA}/\tau_D$.

Pb-FRET method

Both fluorescence imaging and acceptor photobleaching were performed using the Laser Scanning Confocal Microscope system (LSM510/ConfoCor2, Zeiss, Germany). A band-pass fluorescence channel (CH_1) was used to selectively detect the fluorescence from donor, and a long-pass fluorescence channel (CH_2) was used to collect the fluorescence normally from both donor and acceptor. We set C_{D-CH1} as the ratio of fluorescence intensity collected by the first channel (CH_1) to the total fluorescence intensity emitted by donor, and C_{A-CH2} as the ratio of fluorescence intensity collected by the second channel (CH_2) to the total fluorescence intensity emitted by acceptor, and C_{D-CH2} as the ratio of fluorescence intensity collected by CH_2 to the total fluorescence intensity emitted by donor. Therefore,

$$\boldsymbol{C}_{D-CH1} = \int_{\lambda_1}^{\lambda_2} Fil_1(\lambda)\boldsymbol{SP}_d(\lambda)d\lambda \Big/ \int_0^{\infty} \boldsymbol{SP}_d(\lambda)d\lambda \tag{1}$$

$$\boldsymbol{C}_{A-CH2} = \int_{\lambda_3}^{\lambda_4} Fil_2(\lambda)\boldsymbol{SP}_a(\lambda)d\lambda \Big/ \int_0^{\infty} \boldsymbol{SP}_a(\lambda)d\lambda \tag{2}$$

$$\boldsymbol{C}_{D-CH2} = \int_{\lambda_3}^{\lambda_4} Fil_2(\lambda)\boldsymbol{SP}_d(\lambda)d\lambda \Big/ \int_0^{\infty} \boldsymbol{SP}_d(\lambda)d\lambda \tag{3}$$

where $Fil_1(\lambda)$ and $Fil_2(\lambda)$ are the permeate coefficient spectra of the filters used for the CH_1 and CH_2 channels, respectively. and SP_d (λ) and SP_a (λ) are the normalized emission spectra of donor and acceptor, respectively.

Here, we set the excitation laser intensity absorbed by donor is I_0, and that absorbed by acceptor is RI_0, the coefficient R can be obtained by the ratio of absorbance coefficients of acceptor to donor at the excitation wavelength. We set that the FRET efficiency of FRET pair is E, and G_D and G_A are the gain coefficients for CH_1 and CH_2 fluorescence detection channels, respectively (Fig. 1 [18]).

Before photobleaching acceptor, I_D, the fluorescence intensity in CH_1 channel, accounts for the fluorescence intensity from donor alone due to direct excitation and FRET, thus

$$\boldsymbol{I}_D = \boldsymbol{I}_0\phi_D(1-E)\boldsymbol{C}_{D-CH1}\boldsymbol{G}_D \tag{4}$$

The fluorescence intensity I_A in CH_2 channel normally includes three parts of fluorescence: FRET, the direct excitation of acceptor and the donor emission bleed , so I_A can be expressed as

$$\boldsymbol{I}_A = [\boldsymbol{I}_0\phi_D\boldsymbol{E}\phi_A\boldsymbol{C}_{A-CH2} + R\boldsymbol{I}_0\phi_A\boldsymbol{C}_{A-CH2} + \boldsymbol{I}_0\phi_D(1-E)\boldsymbol{C}_{D-CH2}]\boldsymbol{G}_A \tag{5}$$

All data were normalized to 100 in arbitrary unit at the start point of bleaching, thus I_D and I_A are equal at the start point of bleaching as shown in Fig. 2d, therefore

$$\frac{\boldsymbol{I}_0\phi_D(1-E)\boldsymbol{C}_{D-CH1}\boldsymbol{G}_D}{[\boldsymbol{I}_0\phi_D\boldsymbol{E}\phi_A\boldsymbol{C}_{A-CH2} + \boldsymbol{R}\boldsymbol{I}_0\phi_A\boldsymbol{C}_{A-CH2} + \boldsymbol{I}_0\phi_D(1-E)\boldsymbol{C}_{D-CH2}]\boldsymbol{G}_A} = 1 \tag{6}$$

The acceptor in the chosen region of cells expressing FRET plasmid was selectively photobleached with the maximum dose of photobleaching laser line. Selectively

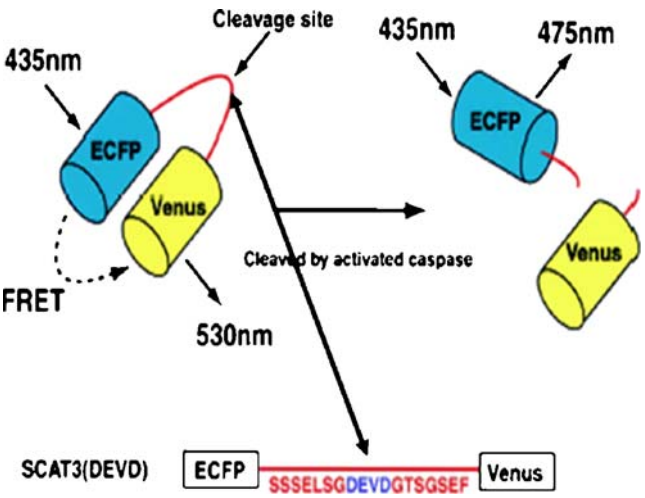

Fig. 1 Schematic representation of SCAT3 [18]. SCAT3 consists of a donor (enhanced cyan fluorescent protein, ECFP) and an acceptor (Venus, a mutant of yellow fluorescent protein). The linking sequence contains a caspase-3 cleavage, DEVD. The activated caspase-3 should cleave the linker and lead to a significant reduction of FRET efficiency

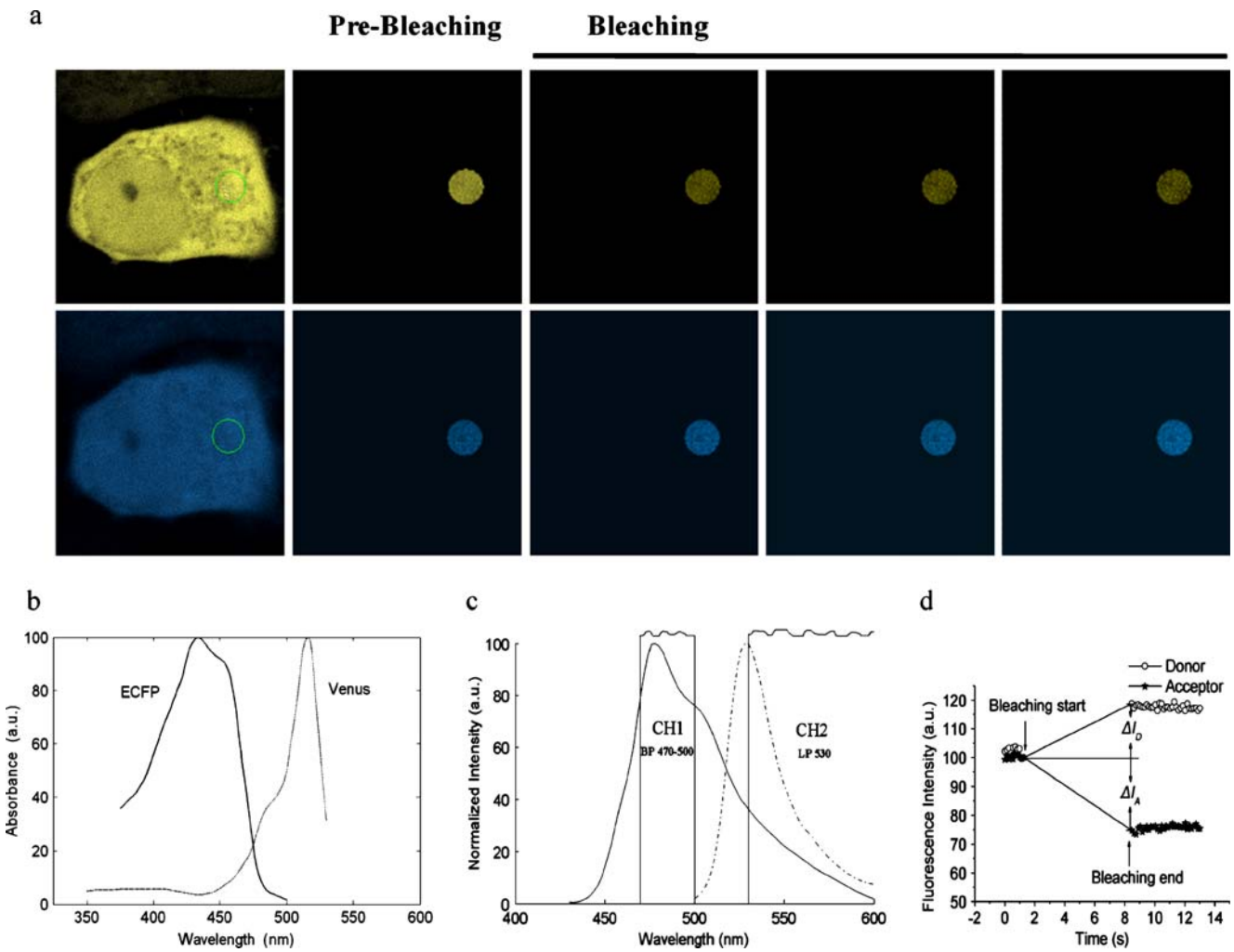

Fig. 2 Fluorescence intensity in both donor (CH_1) and FRET ($CH2$) channels during selectively photobleaching acceptor. **a** Confocal fluorescence images of ECFP and Venus. The acceptor (Venus) was photobleached by the maxium 514-nm laser in the ROI pattern corresponding to the circle area. The fluorescence intensity of ECFP channel (CH_1) increases during photobleaching Venus (CH_2). **b** the absorption spectra of ECFP and Venus. **c** The emission spectra of ECFP and Venus, and the spectra of filters used for Confocal fluorescence images, 470–500 nm band-pass for ECFP channel (CH_1), 530 nm long-pass for Venus channel (CH_2). **d** The fluorescence intensity of ECFP and Venus channels before and during acceptor photobleaching. The fluorescence intensity in CH_1 and CH_2 at the start of bleaching was normalized to 100 in arbitrary unit. ΔI_D was the increased intensity of donor. ΔI_A was the decreased intensity of acceptor at the end of bleaching

photobleaching acceptor leads to a decrease of the fluorescence intensity in CH_1 and an increase of the fluorescence intensity in CH_2. After photobleaching acceptor, the decreased excitation laser directly to excite acceptor is $R^{\triangle}I$, and the decreased absorption of acceptor due to FRET is $^{\triangle}I\varphi_D E$. We set the increased fluorescence intensity in CH_1 channel as ΔI_D , and the decreased fluorescence intensity in CH_2 channel as $^{\triangle}I_A$, therefore

$$\Delta \boldsymbol{I}\phi_D \boldsymbol{E}\boldsymbol{C}_{D-CH1}\boldsymbol{G}_D = \Delta \boldsymbol{I}_D \tag{7}$$

$$(\Delta \boldsymbol{I}\phi_D \boldsymbol{E}\phi_A \boldsymbol{C}_{A-CH2} + \boldsymbol{R}\Delta \boldsymbol{I}\phi_A \boldsymbol{C}_{A-CH2} - \Delta \boldsymbol{I}\phi_D \boldsymbol{E}\boldsymbol{C}_{D-CH2})\boldsymbol{G}_A = \Delta \boldsymbol{I}_A \tag{8}$$

In this study, the FRET plasmid is SCAT3, and 458 nm laser from an Argon ion laser is used for ECFP excitation. Zeiss Plan-Neofluar 40 × oil immersion objective lens (NA=1.45) is used. Images are acquired through ECFP (CH_1) and Venus (CH_2) filter channels, respectively. The emission fluorescence channels are 470–500 nm band-pass for donor ECFP (CH_1), 530 nm long-pass (CH_2) for the acceptor Venus. The acceptor (Venus) in the chosen region inside the living cells stably expressing SCAT3 is selectively bleached with the maximum of 514 nm laser line. Figure 2a shows the images obtained by ROI (region of interesting) mode in LSCM during photobleaching. Figure 2b shows the absorption spectra of ECFP and Venus. As the

absorbance coefficients of ECFP at 434 nm and Venus at 515 nm are 32500 $M^{-1}cm^{-1}$ [31] and 92200 $M^{-1}cm^{-1}$, respectively [32], the absorbance coefficients of ECFP and Venus at 458 nm are 27500 $M^{-1}cm^{-1}$ and 8125 $M^{-1}cm^{-1}$ can be obtained from the absorption spectra, and the coefficient R is 0.29. Figure 2c shows the emission spectra of ECFP and Venus, and the filter spectra of CH_1 and CH_2. The fluorescence intensities of ECFP and Venus channels before and during photobleaching acceptor are shown in Fig. 2d. The $Fil_1(\lambda)$ and $Fil_2(\lambda)$ for our system approximate to 1, substituting the standard emission spectra data of ECFP and Venus into Eqs. (1), (2) and (3), we get

$$\boldsymbol{C}_{D-CH1} = \int_{470}^{500} \boldsymbol{SP}_d(\lambda)d\lambda / \int_{430}^{600} \boldsymbol{SP}_d(\lambda)d\lambda = 0.44 \tag{9}$$

$$\boldsymbol{C}_{A-CH2} = \int_{530}^{600} \boldsymbol{SP}_a(\lambda)d\lambda / \int_{500}^{600} \boldsymbol{SP}_a(\lambda)d\lambda = 0.67 \tag{10}$$

$$\boldsymbol{C}_{D-CH2} = \int_{530}^{600} \boldsymbol{SP}_d(\lambda)d\lambda / \int_{430}^{600} \boldsymbol{SP}_d(\lambda)d\lambda = 0.18 \tag{11}$$

The quantum yields of ECFP and Venus are $\varphi_D = 0.40$ [31] and $\varphi_A = 0.57$ [32]. Substituting Eqs. (9), (10), (11) and R, φ_D, φ_A into Eqs. (6), (7) and (8), and we can get

$$\boldsymbol{E}^2(0.08\Delta\boldsymbol{I}_A + 0.08\Delta\boldsymbol{I}_D) + \boldsymbol{E}(0.18\Delta\boldsymbol{I}_A + 0.03\Delta\boldsymbol{I}_D) = 0.11\Delta\boldsymbol{I}_D \tag{12}$$

From Eq.12, the FRET efficiency E is:

$$E = \frac{-(18\Delta\boldsymbol{I}_A + 3\Delta\boldsymbol{I}_D) + \sqrt{(18\Delta\boldsymbol{I}_A + 3\Delta\boldsymbol{I}_D)^2 + 352\Delta\boldsymbol{I}_D(\Delta\boldsymbol{I}_A + \Delta\boldsymbol{I}_D)}}{16(\Delta\boldsymbol{I}_A + \Delta\boldsymbol{I}_D)} \tag{13}$$

When E is less than 0.3, E^2/E <0.3, $^{\triangle}I_A$ is normally much bigger than $^{\triangle}I_D$. In this case, the FRET efficiency E can be simply obtained by

$$E = \frac{11\Delta\boldsymbol{I}_D}{18\Delta\boldsymbol{I}_A + 3\Delta\boldsymbol{I}_D} \tag{14}$$

If we get $^{\triangle}I_D$ and $^{\triangle}I_A$ by photobleaching acceptor, the FRET efficiency can be quickly obtained by Eq.13 or 14.

Statistical analysis

Results are expressed as mean ± standard deviation (SD). Student's *t*-test is used to compare the mean differences between samples using the statistical software SPSS version 10.0 (SPSS, Chicago). Throughout this work, it is considered to be statistically significant when P value is less than 0.05.

Results

Inhibition of cell viability and activation of caspase-3 by STS

The effect of STS on the cell viability was assessed using CCK-8. Cells were treated with 1 μmol/L of STS for 0, 6 or 12 h, respectively. Figure 3a showed that the cell viability decreased with increasing time of STS treatment. The OD_{450} values of cells under STS treatment for 0, 6, 12 h were 2.14±0.02, 1.66±0.07, 0.84±0.05 (n=4), respectively. These results demonstrated that STS inhibited the cell viability in a time-dependent manner. To verify whether caspase-3 was involved in STS induced-cell death, western blot assay was performed (Fig. 3b), and demonstrated that STS induced caspase-3 activation in a time-dependent manner.

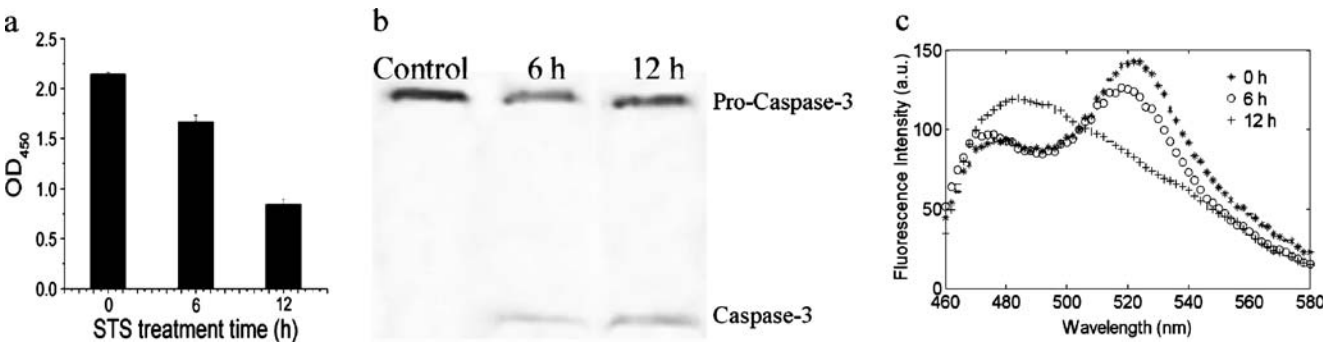

Fig. 3 Inhibition of STS on cell viability in ASTC-a-1cells. The cells were treated by 1 μmol/L STS for 0, 6, or 12 h. The cell viability was measured by the cell counting kit method (CCK-8). * denotes P<0.05. Data were analyzed with the SPSS10.0 software. **b** The Western blot assay signals were detected by an ODYSSEY1 Infrared Imaging System. Cell used for Western blot assay were treated with STS for 0, 6 or 12 h. **c** The emission spectra of SCAT3 inside living cells obtained by auto-microplate reader after cell were treated by STS for 0, 6, or 12 h after STS, respectively. The excitation wavelength for SCAT3 was 409–427 nm and the emission fluorescence channel was 454–600 nm band-pass

The emission spectra of the SCAT3 were acquired at 0, 6, or 12 h after STS treatment using auto-microplate reader (infinite M200, Tecan, Austria) as in our previous study [28]. The excitation wavelength for SCAT3 was 398–438 nm while its emission fluorescence was detected by a 460–600 nm band-pass filter. As shown in Fig. 3c, bimodal emission peaks at 480 and 526 nm were observed inside living healthy cells expressing SCAT3 before the cells were treated with STS. The strong peak at 526 nm of Venus was due to the FRET between ECFP and Venus. The peak at 526 nm gradually decreased after STS treatment, and completely disappeared at 12 h after STS treatment, while the peak of 476 nm increased to the maximum, implying that STS activated caspase-3, which in turn cleaved SCAT3, and leading to the loss of the FRET efficiency of SCAT3.

Pb-FRET method is independent of bleaching degree

To analyze the influence of bleaching degree on the FRET efficiency obtained by Pb-FRET, the Venus of SCAT3 in different ROIs inside living cells expressing stably SCAT3 was photobleached for various photobleaching times. The ratio of $\Delta I_A/100$ was used to define the bleaching degree. The fluorescence intensities at various bleaching degrees of 30%,40%,50% and 60% were shown in Fig. 4a–d, and the FRET efficiencies of SCAT3 inside living cells have no noticeable change under different photobleaching degrees (Fig. 4e,). These results showed that Pb-FRET method is independent of bleaching degree. Thus we can conveniently obtain the FRET efficiency at less bleaching degree by a short bleaching, which has little damage to the living.

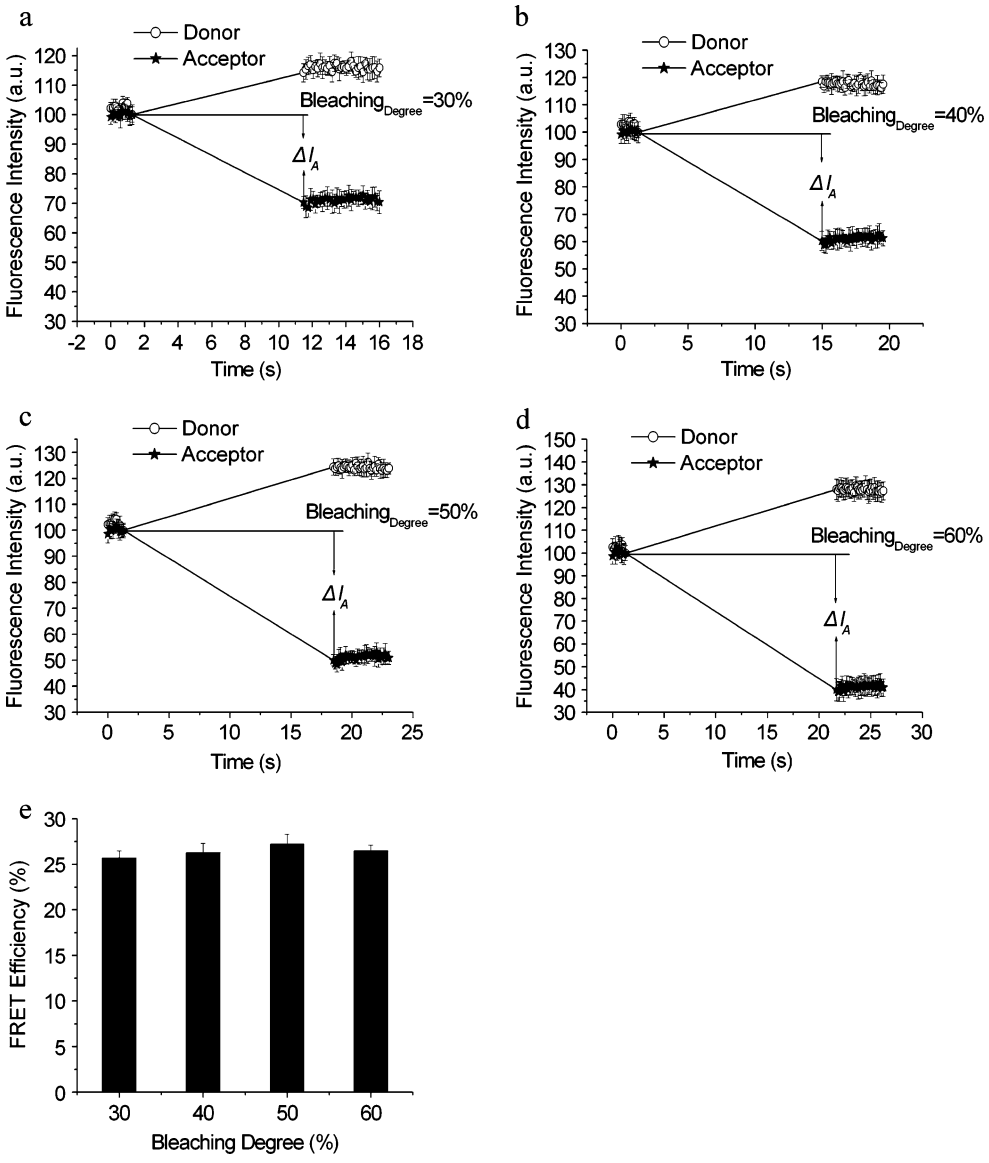

Fig. 4 The fluorescence intensity in CH_1 and CH_2 under varying bleaching degree with 30%(**a**), 40%(**b**), 50 %(**c**), and 60%(**d**). (**e**) The FRET efficiency obtained by Pb-FRET corresponding to (**a**)–(**d**). The results have no noticeable difference at different photobleaching degrees for the cells stably expressing SCAT3 under normal condition

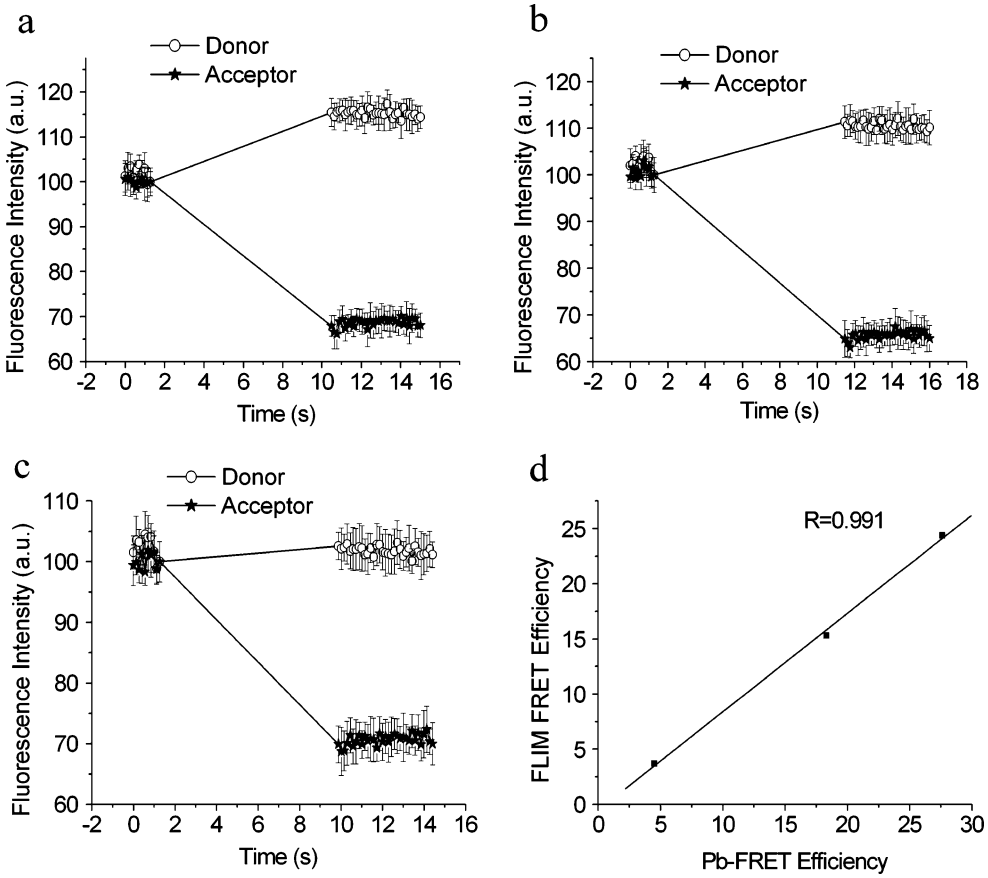

Fig. 5 Quantitative Pb-FRET analysis of the SCAT3 FRET efficiency after STS treatment. **a**–**c** The fluorescence intensity in CH_1 and CH_2 before and after photobleaching acceptor corresponding to 0, 6 or 12 h after STS treatment. **d** Correlation analysis of the FRET efficiency obtained by Pb-FRET and by FLIM-FRET. The Pb-FRET efficiency and FLIM-FRET efficiency was highly correlated (the correlation coefficient R=0.991)

Monitoring dynamic of the FRET efficiency of SCAT3 in single living cells by Pb-FRET method during STS-induced apoptosis

Photobleaching Venus, the acceptor of SCAT3, was performed inside living cells stably expressing SCAT3 at 0, 6, or 12 h after STS treatment (Fig. 5a). We found that the fluorescence intensity in CH_1 channel increased to about 120 (in arbitrary unit), while the fluorescence intensity in CH_2 channel decreased to about 65 (in arbitrary unit), implying that there were noticeable FRET between ECFP and Venus of SCAT3 in the control living cells. At 6 and 12 h after STS treatment, the fluorescence intensity in CH_1 channel increased to about 115 (Fig. 5b) and 105 (Fig. 5c) (in arbitrary unit), but that in CH_2 channel decreased to about 63 (Fig. 5b) and 70 (Fig. 5c) (in arbitrary unit) after photobleaching acceptor. The increase of fluorescence intensity in ECFP channel (CH_1) was not noticeable after Venus was bleached (Fig. 5c) compare with that in Fig. 5a, implying that STS activated caspase-3, which in turn cleaved SCAT3. Our quantitative analysis of the SCAT3 FRET efficiency in living cells by Pb-FRET method was shown in Table 1, the FRET efficiency was about 25.5% in control healthy living cells, and it decreased to about 16.7% and 4.5% at 6 and 12 h after STS treatment, implying that STS induced time-dependent caspase-3 activation.

FLIM was used to further validate the Pb-FRET method. In the cells expressing ECFP alone, the mean fluorescence lifetime of ECFP over the whole cell was 2.45 ns, which was consistent with previous results [27, 28]. In comparison, the mean fluorescence lifetime of ECFP in the cells stably expressing SCAT3 was 1.85 ns (control). The lifetime of ECFP, the donor of SCAT3, increased from 1.85 ns to 2.05 ns or 2.33 ns at 6 h or 12 h after STS treatment, respectively. The corresponding FRET efficiency decreased from 24.4% (control) to 15.3% (6 h) or 3.7% (12 h), respectively. The fluorescence lifetimes of ECFP from 40–50 different cells in at least three independent experiments were listed in Table 1. The FRET efficiency obtained by FLIM method was in good agreement with that obtained by Pb-FRET method, and the correlation coeffi-

Table 1 FRET efficiency of SCAT3 obtained by Pb-FRET and FLIM after STS treatment

STS Treatment Time (h)	Pb-FRET Efficiency (%)	FLIM FRET Efficiency (%)
0	25.5±1.7	24.4±0.9
6	16.7±2.1	15.3±0.7
12	4.5±1.0	3.7±0.6

cient between the Pb-FRET method and FLIM FRET efficiency was 0.991 (Fig. 5d).

Discussions and conclusions

When and where proteins associate with each other in living cells are essential questions in many biological processes. Real-time quantitative analysis of FRET microscopy techniques has recently become extremely important for monitoring the dynamics of protein-protein interactions in living cells. However, excitation and emission spectral crosstalks make it very difficult to quantitatively analyze FRET efficiency in living cells. Although the Pb-FRET method eliminates the excitation spectral crosstalks and the emission spectral bleed of donor into the FRET channel (CH_2), it has two requirements: the first detection channel (CH_1) selectively collects fluorescence only from donor, and photobleaching laser can selectively photobleach acceptor. Fortunately, the two requirements of Pb-FRET method can be easily performed on current confocal laser scanning fluorescence microscope (CLSFM) for most of the FRET pairs based on green fluorescent proteins (GFPs), such as ECFP-EYFP, ECFP-Venus, ECFP-EGFP, ECFP-RFP, EGFP-RFP, and Venus-RFP.

The emission crosstalk can be linearly corrected for measuring FRET efficiency. In this study, we introduced the coefficient C_{D-CH1}, C_{A-CH2} and C_{D-CH2} to correct the artifacts due to crosstalks in acceptor fluorescence channel, and developed a novel algorithm for selectively photobleaching acceptor that accounts for FRET activity. For this method, what we concerned about was the fluorescence intensities of donor and acceptor at the acceptor bleaching start and end points. Therefore the fluorescence recovery after photobleaching (FRAP) would have no influence on the FRET efficiency detection. Equation 4 used the initial normalized intensity at the bleaching start point. Equations (5) and (6) consider the decrease of fluorescence intensity from acceptor, and the increase of fluorescence intensity from donor at bleaching end point. Only the bleached acceptors contribute to the intensity changes, and the unbleached acceptors have no influence on the change of fluorescence intensity in both CH_1 and CH_2 channels. Therefore the Pb-FRET method is independent of the bleaching degree. Due to these advantages, Pb-FRET method can detect FRET efficiency at second time-scale, and even at microsecond time-scale when combined with spot photobleaching [33], which makes it convenient to quantitatively monitor FRET efficiency in real-time inside single living cells.

Two-photon excitation FLIM was used to validate Pb-FRET method in this study. FLIM-FRET exploits the decrease of donor lifetime due to FRET, so the significant advantage of FLIM-FRET is free to spectral detection crosstalks and fluophor concentration. However, several processes can contribute to the decrease in fluorescence lifetime and invalidate FRET measurements. The first is photobleaching, which should decrease the lifetime of donor during measurement, resulting in over-estimated FRET efficiencies. The second is photoconversion which might erroneously contribute to FRET. Irradiation of donor and acceptor might induce a photochemical reaction of chromophore that yielded an isomer with a shorter fluorescence lifetime. Pb-FRET is based on the selectively photobleaching acceptors and the fluorescence intensity data of donor and acceptor at the start and end points of bleaching acceptor, thus Pb-FRET is not suffered from photobleaching and photoconversion.

Traditional intensity-based FRET requires multiple sets of images with varying excitation and detection conditions, as well as with reference samples that contain only one of the fluorophores [10, 11, 34, 35]. In this process, the fluorescence intensity of donor in the absence (I_D) and presence (I_{DA}) of acceptor should be measured, with the FRET efficiency being $E = 1\text{-}I_{DA}/I_D$. In order to detect I_D , it is necessary to take very long time to photobleach all of the acceptors, which may cause serious damage to living cells. Therefore, although this photobleaching acceptor is an alternative method avoiding these complex correction schemes, it is not suitable for measuring FRET efficiency inside living cells in real-time. Compared with those intensity-based FRET methods, the data analysis of Pb-FRET does not need to perform a large number of negative controls and some very difficult corrections. Furthermore, the temporal resolution of Pb-FRET method is in second time-scale for ROI photobleaching, and even in microsecond time-scale for spot photobleaching, so Pb-FRET method may be used to quantitatively monitor the FRET efficiency in real-time. More importantly, Pb-FRET method is not influenced by FRAP. These advantages make Pb-FRET method have great potential to quantitatively detect protein-protein interactions in living cells.

Acknowledgements We thank Prof. M. Miura for providing us with the *SCAT3* plasmid. This study was supported by National Natural Science Foundation of China (Grant No. 30670507 and 60627003), the Natural Science Foundation of Guangdong Province (F051001), "Shuguang Scholor" (Grant No. 07SG05) of Education Commision and "Leading Academic Development Project" (Grant No. B109) of the Science & Technology Commission of Shanghai Municipality.

References

1. Lakowicz JR (1999) Principles of fluorescence spectroscopy. Plenum, NewYork
2. Förster T (1948) Intermolecular energy migration and fluorescence. Ann Phys 6:55–75. doi:10.1002/andp. 19484370105

3. Stryer L, Haugland R (1967) Energy transfer: a spectroscopic ruler. Proc Natl Acad Sci USA 58:719–726. doi:10.1073/pnas. 58.2.719
4. Gordon GW, Berry G, Liang XH, Levine B, Herman B (1998) Quantitative fluorescence resonance energy transfer measurements using fluorescence microscopy. Biophys J 74:2702–2713. doi:10.1016/S0006-3495(98)77976-7
5. Jares-Erijman EA, Jovin TM (2003) FRET imaging. Nat Biotechnol 21:1387–1395. doi:10.1038/nbt896
6. Chen Y, Periasamy A (2006) Intensity range based quantitative FRET data analysis to localize protein molecules in live cell nuclei. J Fluoresc 16:95–104. doi:10.1007/s10895-005-0024-1
7. Becker W, Bergmann A, Hink MA, König K, Benndorf K, Biskup C (2004) Fluorescence lifetime imaging by time-correlated single-photon counting. Microsc Res Tech 63:58–66. doi:10.1002/jemt.10421
8. Hoppe A, Christensen K, Swanson JA (2002) Fluorescence resonance energy transfer-based stoichiometry in living cells. Biophys J 83:3652–3664. doi:10.1016/S0006-3495(02)75365-4
9. Pelet S, Previte MJR, So PTC (2006) Comparing the quantification of Förster resonance energy transfer measurement accuracies based on intensity, spectral, and lifetime imaging. J Biomed Opt 11:034017. doi:10.1117/1.2203664
10. Kenworthy AK (2002) Imaging protein-protein interactions using fluorescence resonance energy transfer microscopy. Methods 24:289–296. doi:10.1006/meth.2001.1189
11. Gu Y, Di WL, Kelsell DP, Zicha D (2004) Quantitative fluorescence resonance energy transfer (FRET) measurement with acceptor photobleaching and spectral unmixing. J Micro 15:162–173. doi:10.1111/j.0022-2720.2004.01365.x
12. Hoffmann B, Zimmer T, Klöcker N, Kelbauskas L, König K, Benndorf K, Biskup C (2008) Prolonged irradiation of enhanced cyan fluorescent protein or Cerulean can invalidate Förster resonance energy transfer measurements. J Biomed Opt 13:031205. doi:10.1117/1.2937829
13. Berney C, Danuser G (2003) FRET or no FRET: a quantitative study. Biophys J 84:3992–4010. doi:10.1016/S0006-3495(03)75126-1
14. Gordon GW, Berry G, Liang XH, Levine B, Herman B (1998) Quantitative fluorescence resonance energy transfer measurements using fluorescence microscopy. Biophys J 74:2702–2713. doi:10.1016/S0006-3495(98)77976-7
15. Xia ZP, Liu YC (2001) Reliable and global measurement of fluorescence energy transfer using fluorescence microscopes. Biophys J 81:2395–2402. doi:10.1016/S0006-3495(01)75886-9
16. Kerr JF, Winterford CM, Harmon BV (1994) Apoptosis: its significance in cancer and cancer therapy. Cancer 73:2013–2026. doi:10.1002/1097-0142(19940415)73:8<2013::AID-CNCR2820730802>3.0.CO;2-J
17. Green DR (1998) Apoptotic pathways: the roads to ruin. Cell 94:695–698. doi:10.1016/S0092-8674(00)81728-6
18. Kiwamu T, Takeharu N, Atsushi M, Masayuki M (2003) Spatio-temporal activation of caspase revealed by indicator that is insensitive to environmental effects. J Cell Biol 160:235–243. doi:10.1083/jcb.200207111
19. Wu YX, Xing D, Chen WR (2006) Single cell FRET imaging for determination of pathway of tumor cell apoptosis induced by photofrin-PDT. Cell Cycle 5:729–734
20. Wu YX, Xing D, Luo SM, Tang YH, Chen Q (2006) Detection of caspase-3 activation in single cells by fluorescence resonance energy transfer during photodynamic therapy induced apoptosis. Cancer Lett 235:239–247. doi:10.1016/j.canlet.2005.04.036
21. Wu YY, Xing D, Chen WR, Wang XC (2007) Bid is not required for Bax translocation during UV-induced apoptosis. Cell Signal 19:2468–2478. doi:10.1016/j.cellsig.2007.07.024
22. Liu L, Xing D, Chen WR, Chen TS, Pei YH, Gao XJ (2008) Calpain-mediated pathway dominates cisplatin-induced apoptosis in human lung adenocarcinoma cells as determined by real-time single cell analysis. Int J Cancer 122:2210–2222. doi:10.1002/ijc.23378
23. Salako MA, Carter MJ, Kass GEN (2006) Coxsackievirus protein 2BC blocks host cell apoptosis by inhibiting caspase-3. J Biol Chem 281:16296–16304. doi:10.1074/jbc.M510662200
24. Rehm M, Düßmann H, Jänicke RU, Tavaré JM, Kögel D, Prehn JH (2002) Single cell fluorescence resonance energy transfer analysis demonstrates that caspase activation during apoptosis is a rapid process: role of caspase-3. J. Biol. Chem. 277:24506–24514. doi:10.1074/jbc.M110789200
25. Andersson M, Sjöstrand J, Petersen A, Honarvar AKS, Karlsson JO (2000) Caspase and proteasome activity during staurosporine-induced apoptosis in lens epithelial cells. Invest Ophthalmol Vis Sci 41:2623–2632
26. Xue LY, Chiu SM, Oleinick NL (2003) Staurosporine-induced death of MCF-7 human breast cancer cells: distinction between caspase-3-dependent steps of apoptosis and the critical lethal lesions. Exp Cell Res 283:135–145. doi:10.1016/S0014-4827(02)00032-0
27. Pepperkok R, Squire A, Geley S, Bastiaens PI (1999) Simultaneous detection of multiple green fluorescent proteins in live cells by fluorescence lifetime imaging microscopy. Curr Biol 9:269–272. doi:10.1016/S0960-9822(99)80117-1
28. Pan WL, Qu JL, Chen TS, Sun L (2009) FLIM and emission spectral analysis of caspase-3 activation inside single living cell during anticancer drug-induced cell death. Eur Biophys J. doi:10.1007/s00249-008-0390-0
29. Zeng SQ, Lv XH, Zhan C, Chen WR, Xiong WH, Jacuqes SL, Luo QM (2006) Simultaneous compensation for spatial and temporal dispersion of acousto-optical deflectors for two-dimensional scanning with a single prism. Opt Lett 31:1091–1093. doi:10.1364/OL.31.001091
30. Zeng SQ, Li DR, Luo QM (2007) Pulse broadening of the femtosecond pulses in a Gaussian beam passing an angular disperser. Opt Lett 32:1180–1182. doi:10.1364/OL.32.001180
31. Tsien RY (1998) The green fluorescent protein. Annu Rev Biochem 67:509–544. doi:10.1146/annurev.biochem.67.1.509
32. Wei WS (2005) Fluorescent proteins as tools to aid protein production. Microb Cell Fact 4:12. doi:10.1186/1475-2859-4-12
33. Partikian A, Ölveczky B, Swaminathan R, Li YX, Verkman AS (1998) Rapid diffusion of green fluorescent protein in the mitochondrial matrix. J Cell Biol 140:821–829. doi:10.1083/jcb.140.4.821
34. Elangovan M, Wallrabe H, Chen Y, Day RN, Barroso M, Eriasam A (2003) Characterization of one- and two-photon excitation fluorescence resonance energy transfer microscopy. Methods 291:58–73. doi:10.1016/S1046-2023(02)00283-9
35. Hoppe A, Christensen K, Swanson JA (2002) Fluorescence resonance energy transfer-based stoichiometry in living cells. Biophys J 83:3652–3664. doi:10.1016/S0006-3495(02)75365-4